Acta Chemica Scandinavica A 30 (1976) 8—14

Magnetic Structures and Properties of $V_{1-t}Mn_tAs$

KARI SELTE,[a] ARNE KJEKSHUS,[a] GUNNAR VALDE,[a] and ARNE F. ANDRESEN[b]

[a] Kjemisk Institutt, Universitetet i Oslo, Blindern, Oslo 3, Norway and [b] Institutt for Atomenergi, Kjeller, Norway

The pseudo-binary VAs – MnAs system has been investigated by X-ray and neutron diffraction and magnetic susceptibility measurements. VAs and MnAs are completely soluble in each other and the crystal structure at and below room temperature is of the MnP type, except for a very small range near the composition MnAs where the NiAs type structure prevails. In the Mn rich region of $V_{1-t}Mn_tAs$ a second or higher order transition from MnP to NiAs type structure is observed at elevated temperatures. The temperature dependence of the magnetic susceptibility follows the Curie-Weiss Law in the region of the (high temperature) NiAs type structure. The low temperature phase with NiAs type structure exhibits ferromagnetism. In the region of the MnP type crystal structure a double, a axis type helimagnetic ordering of the spins is adopted at low temperatures ($\sim 0.60 \leqq t \leqq 0.95$ in $V_{1-t}Mn_tAs$). The spiral parameters depend both on composition and temperature.

Studies on the magnetic properties of phases with the MnP type structure are frequently rendered difficult by the small magnetic moments generally associated with such phases. The existence of cooperative, magnetic phenomena may therefore be difficult to detect and large uncertainties are necessarily attached to the interpretation of the experimental data. On turning to ternary phases it may be possible to improve the conditions somewhat by incorporating elements which carry or induce larger magnetic moments. A suitable element for this purpose is Mn. In line with this, the present paper concerns the magnetic structures and properties of $V_{1-t}Mn_tAs$, the work being greatly stimulated by the findings for $Cr_{1-t}Mn_tAs$ [1,2] and $Mn_{1-t}Fe_tAs$.[3]

EXPERIMENTAL

Samples of VAs and MnAs were made by heating weighed quantities of the elements [99.5 % V (A.D. Mackay), 99.9+ % Mn (The British Drug Houses; crushed powder from the commercial electrolytic grade material), and 99.9999 % As (Koch-Light Laboratories)] in evacuated, sealed quartz tubes, as described in Refs. 3 and 4. VAs and MnAs were mixed in proportions appropriate to the desired ternary compositions and subjected to a first annealing at 850 °C for one week. All samples were crushed and subjected to one or two further annealings for one week at 850 °C, then cooled to 600 °C over two days and finally quenched in ice water.

The experimental details concerning the X-ray and neutron diffraction and magnetic susceptibility measurements have been reported earlier.[5]

RESULTS

(i) *Chemical crystal structures.* The room temperature unit cell dimensions of $V_{1-t}Mn_tAs$ are shown in Fig. 1 as functions of the composition parameter t. The complete mutual solid solubility of VAs and MnAs is brought out in the continuous variation of all unit cell dimensions with t. The possible extension of the homogeneity range of $V_{1-t}Mn_tAs$ to metal/non-metal (atomic) ratios different from 1.00 has not been examined for $t \neq 0$ [4] and 1.[6]

At room temperature the MnP type atomic arrangement is stable in the interval $0 \leqq t \leqq 0.98$, whereas the NiAs type prevails for $0.98 < t \leqq 1$ (see Figs. 1 and 2). The X-ray and neutron diffraction data show that the substituted atoms are distributed at random in the metal sub-lattice, unit cell dimensions and positional parameters for $t = 0.50$, 0.60, 0.70, 0.90, and 0.95 being given in Table 1.

Table 1. Unit cell dimensions and positional parameters with standard deviations for some $V_{1-t}Mn_tAs$ samples as derived by least squares profile refinements of neutron diffraction data. (Space group *Pnma*; positions 4(*c*); overall profile reliability factors ranging between 0.035 and 0.052.)

t	T (K)	a (Å)	b (Å)	c (Å)	x_T	z_T	x_X	z_X
0.95	80	5.585(1)	3.500(1)	6.181(1)	0.0068(32)	0.2083(21)	0.1992(9)	0.5827(12)
	293	5.703(1)	3.625(1)	6.331(1)	0.0035(11)	0.2171(9)	0.2170(5)	0.5804(8)
0.90	4.2	5.616(1)	3.499(1)	6.210(1)	0.0078(15)	0.2167(45)	0.1957(9)	0.5804(12)
	80	5.619(1)	3.507(1)	6.215(1)	0.0003(19)	0.2062(23)	0.2022(8)	0.5811(10)
	293	5.710(1)	3.601(1)	6.318(2)	0.0025(20)	0.2120(18)	0.2141(7)	0.5868(10)
0.70	4.2	5.652(1)	3.462(1)	6.230(1)	0.0090(20)	0.2085(20)	0.2020(8)	0.5783(8)
	80	5.658(1)	3.465(1)	6.235(1)	0.0103(18)	0.2060(19)	0.2001(9)	0.5766(10)
	293	5.721(1)	3.525(1)	6.296(1)	0.0070(21)	0.2051(18)	0.2095(7)	0.5807(7)
0.60	5	5.683(2)	3.445(2)	6.254(2)	−0.0002(22)	0.1984(22)	0.2038(7)	0.5748(8)
	80	5.691(3)	3.451(2)	6.283(3)	−0.0015(28)	0.1951(27)	0.2054(9)	0.5760(9)
	293	5.735(3)	3.489(2)	6.311(3)	−0.0013(21)	0.2012(21)	0.2071(6)	0.5766(7)
0.50	5	5.709(2)	3.430(1)	6.260(2)	−0.0006(24)	0.1966(24)	0.2013(6)	0.5760(7)
	80	5.714(3)	3.435(2)	6.268(3)	0.0002(27)	0.1983(28)	0.2026(7)	0.5757(8)
	293	5.743(2)	3.464(1)	6.290(2)	0.0017(25)	0.1988(25)	0.2049(7)	0.5759(8)

All pseudo-binary systems of the type TAs $-$MnAs [2,3] contain the unusual feature of taking an NiAs type atomic arrangement as both low (I) and high (II) temperature forms, separated by a temperature interval in which the MnP type structure prevails. This peculiarity is associated with the magnetic behaviour of Mn-rich $T_{1-t}Mn_tAs$ samples; see ii. The second or higher order MnP⇌NiAs (II) type transition in $V_{1-t}Mn_tAs$ has been detected by the high temperature powder X-ray method ($0.70 \leqq t \leqq 1$; see Fig. 3) as well as the magnetic susceptibility data ($0.80 \leqq t \leqq 1$; see ii). The trend in the data, which are mutually consistent

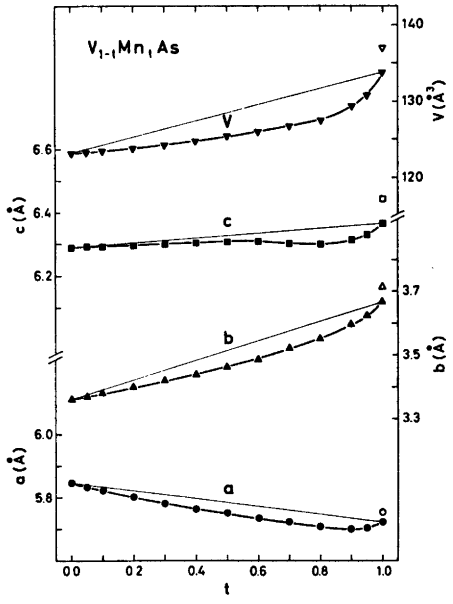

Fig. 1. Room temperature (extrapolated for MnAs) unit cell dimensions of ternary solid solution series VAs−MnAs *versus* composition. Error limits do not exceed size of symbols. Open symbols for MnAs represent data for its NiAs type structure at room temperature.

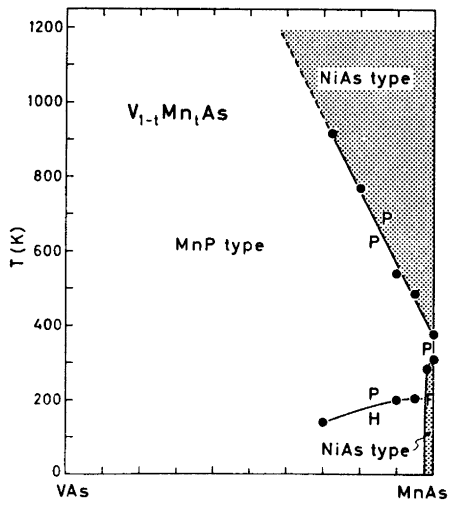

Fig. 2. Diagram of the phase relations in the pseudo-binary VAs−MnAs system. Phase boundaries indicated by broken lines are uncertain. Magnetic state is indicated by: P para, H helical, F ferro.

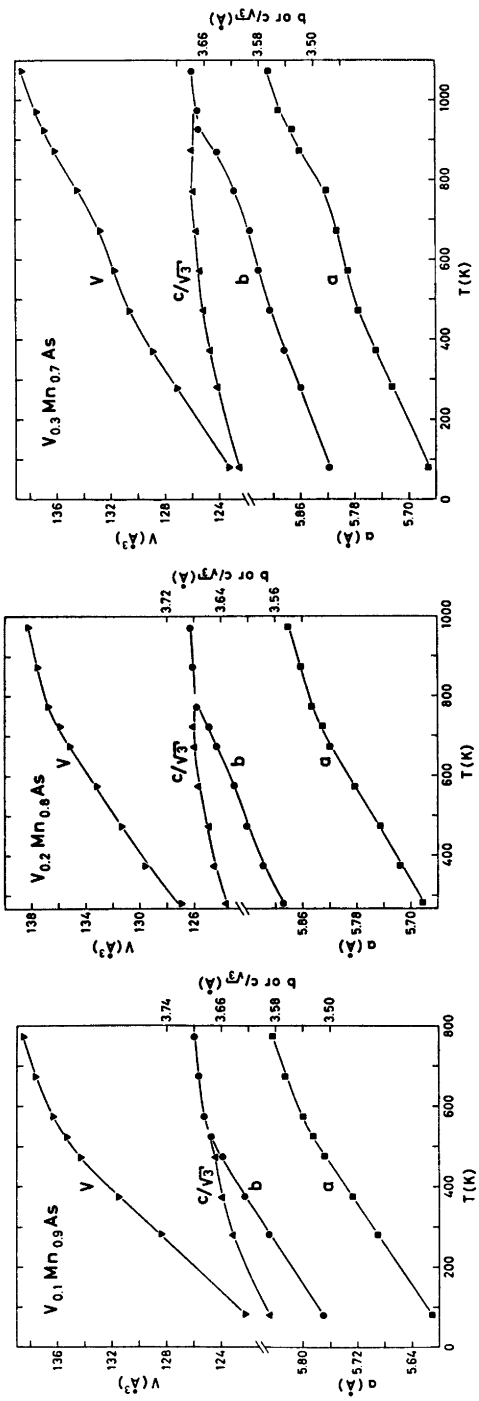

Fig. 3. Unit cell dimensions of three $V_{1-t}Mn_tAs$ samples *versus* temperature. Average relative expansion coefficients α_a [$=\alpha_T - \alpha_{T'}/a_{300}(T-T')$], α_b, α_c multiplied by 10^6 K are 39, 44, 29; 61, 69, 36; and 69, 107, 59 for $V_{0.30}Mn_{0.70}As$ (80 – 700 K), $V_{0.20}Mn_{0.80}As$ (300 – 600 K), and $V_{0.10}Mn_{0.90}As$ (80 – 450 K), respectively.

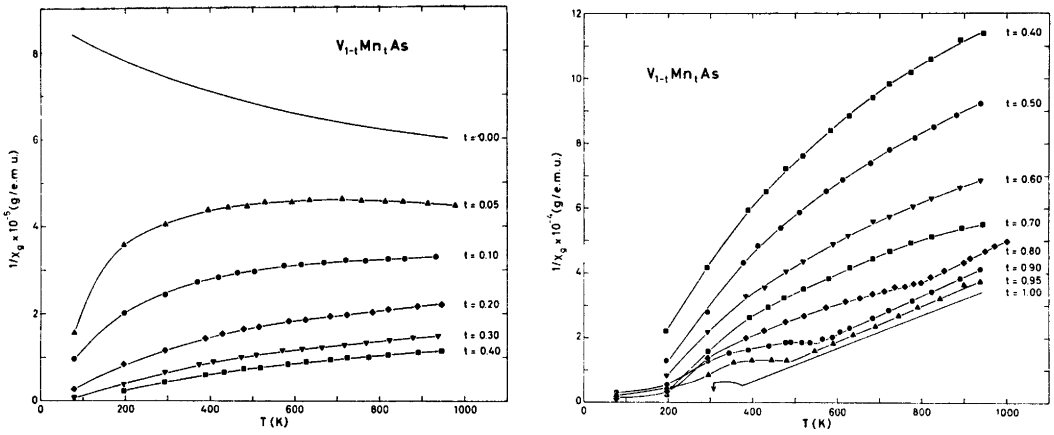

(a) (b)

Fig. 4. Reciprocal magnetic susceptibility as function of temperature for $V_{1-t}Mn_tAs$ samples with (a) $0 \leqq t \leqq 0.40$ and (b) $0.40 \leqq t \leqq 1$. Curves for $t = 0$ and 1 are quoted from Refs. 3 and 4.

for the two sets, suggests that the transition continues to take place in samples with $t < 0.70$, although it could not be followed with our equipment.

Mn-rich $T_{1-t}Mn_tAs$ samples have in common (*cf.* Refs. 2, 3, 7, and 8) a relatively low temperature for the MnP⇌NiAs (II) type transition, an appreciable temperature interval for the complete conversion from the NiAs type to the fully relaxed MnP type positional parameters, and unusually large thermal expansion coefficients in the changing region of the MnP type structure. These phenomena are intimately connected and have probably a common origin in the unique property of Mn, being capable of appreciable adjustments of size as a function of its electronic (*e.g.* high spin/low spin) state.

(ii) *Magnetic susceptibility.* As seen from Fig. 4 the reciprocal magnetic susceptibility *versus* temperature characteristics undergo a gradual change with the composition parameter t of $V_{1-t}Mn_tAs$. Among these thermomagnetic curves, that for $t = 0$ is unique in decreasing steadily with increasing temperature. All the other curves are characterized by having a shorter or longer convex portion towards the temperature axis. For samples with $0.80 \leqq t \leqq 1$ the convex portions are interrupted by linear sections on the high temperature side. The temperature at which the change-over takes place is that for the transition between the MnP and NiAs (II) type structures (see i). Thus, the fulfilment of Curie-Weiss Law is associated with the NiAs type structure. With decreasing content of Mn from $t = 1$ to $t = 0.80$ a small reduction is noted in paramagnetic moment and Curie constant (Table 2).

Non-linear $\chi^{-1}(T)$ curves may almost be taken as a trade mark for phases with the MnP type structure. The $\chi^{-1}(T)$ curves shown in Fig. 4 are no exception in this respect. The thermomagnetic curves for $V_{1-t}Mn_tAs$ show similarities with those for $Cr_{1-t}Mn_tAs$ [2] and $Mn_{1-t}Fe_tAs$,[3] low temperature ferromagnetic behaviour being observed for $t = 1$ and, rather weakly, for $0.40 \leqq t \leqq 0.70$ of the $V_{1-t}Mn_tAs$ phase. (Indication of the weak ferromagnetism was not found in the neutron diffraction data for samples with $t = 0.50$, 0.60, and 0.70.)

(iii) *Magnetic structures.* The ferromagnetic mode of MnAs,[9] with moments arranged

Table 2. Curie constant (θ), paramagnetic moment ($\mu_P = \sqrt{8C_M}$), and number of unpaired electrons ($n = 2S_T$; according to the "spin only" approximation) for $V_{1-t}Mn_tAs$ samples which fulfil Curie-Weiss Law.

t	θ (K)	μ_P (μ_B)	$2S_T$
1.00	270 ± 10	4.5 ± 0.3	3.6 ± 0.2
0.95	255 ± 15	4.3 ± 0.3	3.4 ± 0.2
0.90	240 ± 20	4.2 ± 0.4	3.3 ± 0.3
0.70	230 ± 20	4.0 ± 0.4	3.1 ± 0.3

Table 3. Parameters specifying the double, *a* axis helimagnetic ordering in $V_{1-t}Mn_tAs$. (Angle (β) between moment vector and spiral axis is assumed to be 90°.)

t	0.95	0.90		0.70	
T (K)	80	4.2	80	4.2	80
$\tau/2\pi a^*$	0.128(2)	0.116(2)	0.116(2)	0.080(3)	0.078(3)
μ_T (μ_B)	1.9(1)	1.9(1)	1.9(1)	1.6(1)	1.6(1)
ϕ (°)	65(1)	70(1)	75(1)	60(1)	56(1)
T_N (K)	206(1)	200(1)		142(1)	

perpendicular to the hexagonal *c* axis of its NiAs type atomic arrangement, extends slightly ($t > 0.98$) into the ternary region of $V_{1-t}Mn_tAs$ (*cf.* Fig. 2). The other binary end member, VAs, does not exhibit a cooperative magnetic phenomenon above 4.2 K.[4]

The double, *a* axis type helimagnetic ordering, which rather recently was observed for $Fe_{1-t}Mn_tAs$ ($\sim 0.88 < t < \sim 0.99$; MnP type structure),[3] is also found for $V_{1-t}Mn_tAs$ samples in the interval $\sim 0.60 \leqq t \leqq 0.95$. This helimagnetic mode [3] is, besides the Néel temperature (T_N) and the magnetic moment per metal atom (μ_T), specified by the spiral propagation vector (τ), the phase angle between independent spirals (ϕ), and the angle between the moment and the spiral axis (β). As evident from Fig. 2 and Table 3, T_N varies slowly over the composition range $0.70 \leqq t \leqq 0.95$. A similar statement applies roughly to the magnetic moment when the limited accuracy in the determination of this parameter is considered. For the $V_{0.40}Mn_{0.60}As$ sample, near the Mn-poor limit of the helical mode, T_N is reduced appreciably ($5 < T_N < 80$ K) and the low (almost insignificant) intensity of the magnetic reflections prevents meaningful estimates of the spiral parameters. The propagation vector and the phase angle are found to vary appreciably with composition and temperature (see Fig. 5 and Table 3), thus resembling

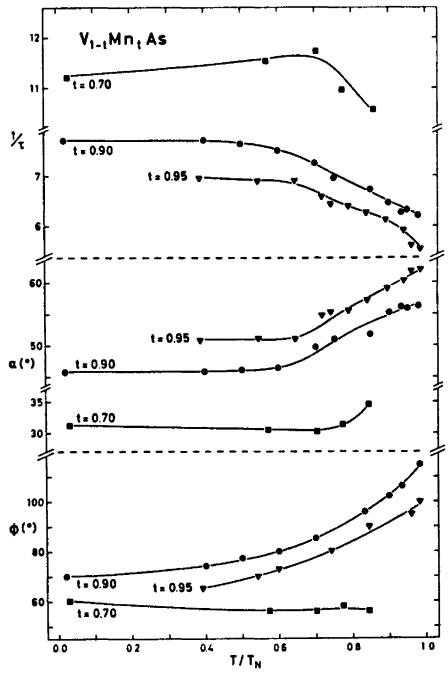

Fig. 5. Spiral turn angle per *a* length (α) and number of *a* lengths per spiral revolution ($1/\tau$) together with phase angle (ϕ) for $t = 0.70$, 0.90, and 0.95 of $V_{1-t}Mn_tAs$ as functions of reduced temperature.

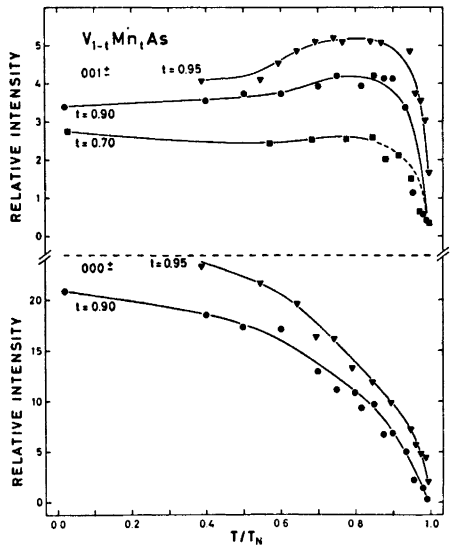

Fig. 6. Temperature dependence of relative, integrated intensities of $000^{\pm}$ and $001^{\pm}$ for $t = 0.70$, 0.90, and 0.95 of $V_{1-t}Mn_tAs$.

to some extent the findings for $Fe_{0.10}Mn_{0.90}As$.[3]

The integrated intensity *versus* reduced temperature relationships for the strongest satellites $000^{\pm}$ and $001^{\pm}$ of $V_{0.05}Mn_{0.95}As$, $V_{0.10}Mn_{0.90}As$ and $V_{0.30}Mn_{0.70}As$ are shown in Fig. 6. (Due to the small value of α for $V_{0.30}Mn_{0.70}As$ $000^{\pm}$ lies extremely close to the primary neutron beam, and the integrated intensity could only be inaccurately determined by subtraction of the background as obtained above T_N.) The marked difference in the temperature variation of the corresponding integrated intensities of $000^{\pm}$ and $001^{\pm}$ immediately suggests that there are changes in ϕ with temperature. The apparent reduction in magnetic moment with temperature for helimagnetic arrangements does not, in general, follow the Brillouin type relationships characteristic of collinear magnetic structures. This is also the case for the double, *a* or *c* axis type spiral structures occurring among the MnP type phases (*cf.* Refs. 3, 5, 10–13), where the disordering of the moments affects the temperature dependences of α, ϕ, and β in addition to μ_T. Lacking a suitable dynamic model for the description of the thermal movements of the moments in terms of the variables μ_T, α, ϕ, and β, the three latter parameters were assumed to be static temperature functions, and the hypothetical $\mu_T/\mu_{T,0K}$ *versus* T/T_N relationship shown in Fig. 7 was postulated. Although the magnetic susceptibility data for $V_{0.30}Mn_{0.70}As$ give indication of a small ferromagnetic component, probably due to deviation of β from 90°, the constraint $\beta = 90°$ was not relaxed. The temperature dependence of α follows from the location of the satellites in relation to the nuclear reflections, permitting this parameter to be established separately. Thus, using the temperature variations of μ_T from Fig. 7, α from Fig. 5, and $\beta = 90°$, the temperature dependence of ϕ shown in the bottom part of Fig. 5 could be deduced from the observed intensities of $000^{\pm}$ and $001^{\pm}$ shown in Fig. 6. As a check of the mutual consistency of the data, the smooth curves in Fig. 6 have been calculated on the deduced spiral parameters, μ_T, α, (β,) and ϕ. The calculated curves are seen to fit the experimental points remarkably well.

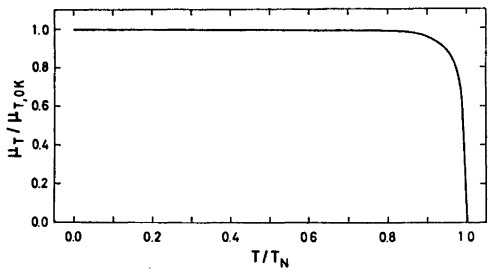

Fig. 7. Postulated temperature dependence of magnetic moments in helimagnetic modes of $V_{0.30}Mn_{0.70}As$, $V_{0.10}Mn_{0.90}As$, and $V_{0.05}Mn_{0.95}As$.

The carefully collected intensity data for $000^{\pm}$ at various temperatures were examined in order to unveil possible sample inhomogeneities of the type encountered for the magnetically isostructural $Mn_{0.90}Fe_{0.10}As$.[3] No such inhomogeneity was found for the $V_{1-t}Mn_tAs$ samples.

DISCUSSION

The phase diagram of the pseudo-binary VAs–MnAs system (Fig. 2) shows marked similarities to that of CrAs–MnAs,[2] but differs to some extent from that of MnAs–FeAs.[3] Since V and Cr precede Mn in the 3*d* series, it would be of interest to examine the phase relationships in the system MnAs–CoAs, where Co, like Fe, succeeds Mn.

The common feature of the high temperature portions of the CrAs–MnAs [2] and VAs–MnAs systems is the second or higher order crystallographic transitions between MnP and NiAs type structures. Similar MnP⇌NiAs type transitions are also found in a number of other binary and ternary phases.[13–17] Available information concerning such transitions are reasonably consistent with recent considerations on geometrical [15] and group theoretical [18] basis.

On substitution of another metal or nonmetal component into a binary MnP type compound which takes cooperative magnetic ordering, two different situations arise. If neither the solute nor the solvent metal atom is Mn, only small substitutions appear to destroy the cooperative magnetic phenomena.[17] Relatively large magnetic homogeneity ranges have, on the other hand, been observed for the pseudo-binary *T*As–MnAs systems studied so far.[2,3]

The magnetic data for the $T_{1-t}Mn_tAs$ phases (as well as $MnP_{1-x}As_x$) also have a number

of other features in common. Whenever the NiAs type structure occurs, the magnetic moments are appreciably higher than found for the corresponding MnP type state (3.1 – 3.7 *versus* 1.3 – 1.9 for the spin quantum number $2S_T$; Ref. 3 and *vide supra*). The terminology high spin/low spin may be used although these phrases have lost their clear-cut meaning here, where the electrons are, at least partly, delocalized and spread over a number of energy bands.

A theoretical investigation of the double, *a*-axis type helimagnetic mode is required in order to compare $V_{1-t}Mn_tAs$ and $Fe_{1-t}Mn_tAs$[3] in a meaningful manner. The starting point of Kallel *et al.*[19] may constitute a suitable basis for such an exploration.

Although $V_{1-t}Mn_t$ As ($\sim 0.60 \leqq t \leqq 0.95$), and $Fe_{1-t}Mn_tAs$ ($\sim 0.88 < t < \sim 0.99$)[3] are magnetically isostructural, the tendency towards conical deformation of the spiral arrangement is more prominent in the latter phase. In neither of the cases conical deformation is observed near the Mn-rich phase boundaries. In order to obtain more insight into the origin of the conical arrangements, attention should be focussed on the behaviour of these phases in magnetic fields.

Acknowledgement. The assistance of Ing. Stanislav Vratislav (I.A.E.A.-fellow from The Technical University of Prague, Czechoslovakia) in some of the neutron diffraction measurements is greatly appreciated.

REFERENCES

1. Watanabe, H., Kazama, N., Yamaguchi, Y. and Ohashi, M. *J. Appl. Phys. 40* (1969) 1128.
2. Kazama, N. and Watanabe, H. *J. Phys. Soc. Jap. 30* (1971) 1319.
3. Selte, K., Kjekshus, A. and Andresen, A. F. *Acta Chem. Scand. A 28* (1974) 61.
4. Selte, K., Kjekshus, A. and Andresen, A. F. *Acta Chem. Scand. 26* (1972) 4057.
5. Selte, K., Kjekshus, A. and Andresen, A. F. *Acta Chem. Scand. 26* (1972) 3101.
6. Grønvold, F., Snildal, S. and Westrum, E. F. *Acta Chem. Scand. 24* (1970) 285.
7. Selte, K. and Kjekshus, A. *Acta Chem. Scand. 27* (1973) 3195.
8. Selte, K., Kjekshus, A. and Andresen, A. F. *Acta Chem. Scand. 27* (1973) 3607.
9. Bacon, G. E. and Street, R. *Nature (London) 175* (1955) 518.
10. Boller, H. and Kallel, A. *Solid State Commun. 9* (1971) 1699.
11. Felcher, G. P., Smith, F. A., Bellavance, D. and Wold, A. *Phys. Rev. B 3* (1971) 3046.
12. Selte, K., Kjekshus, A., Oftedal, T. A. and Andresen, A. F. *Acta Chem. Scand. A 28* (1974) 957.
13. Selte, K., Hjersing, H., Kjekshus, A. and Andresen, A. F. *Acta Chem. Scand. A 29* (1975) 312.
14. Ido, H. *J. Phys. Soc. Japan 25* (1968) 1543.
15. Selte, K. and Kjekshus, A. *Acta Chem. Scand. 27* (1973) 3195.
16. Franzen, H. F. and Wiegers, G. A. *J. Solid State Chem. 13* (1975) 114.
17. Selte, K., Hjersing, H., Kjekshus, A., Andresen, A. F. and Fischer, P. *Acta Chem. Scand. A 29* (1975) 695.
18. Franzen, H. F., Haas, C. and Jellinek, F. *Phys. Rev. B 10* (1974) 1248.
19. Kallel, A., Boller, H. and Bertaut, E. F. *J. Phys. Chem. Solids 35* (1974) 1139.

Received June 2, 1975.